Journal of Cultural Heritage 74 (2025) 265–275

Contents lists available at ScienceDirect

Journal of Cultural Heritage

journal homepage: www.elsevier.com/locate/culher

Original article

Multi-analytical approach for identification of early artificial ultramarine, made by Raimondo di Sangro, in the blue frame on the altar of the Sansevero Chapel Museum in Naples

Gioacchino Tempesta[a,b,*], Alessandro Monno[a,b], Francesco Paolo de Ceglia[c], Andrea Maraschi[d], Elena C.L. Rigante[e], Cosima Damiana Calvano[b,e,f], Giancarlo Capitani[g]

[a] Department of Earth and Geoenvironmental Sciences, University of Bari Aldo Moro, via Orabona, 4, 70125 Bari, Italy
[b] Interdepartmental Centre "Research Laboratory for the Diagnostics of Cultural Heritage", University of Bari Aldo Moro, via Orabona, 4, 70125 Bari, Italy
[c] Interuniversity Research Center "Seminario di Storia della Scienza", Department Dirium, University of Bari Aldo Moro, Piazza Umberto I 1, 70122 Bari, Italy
[d] Department of Literary, Linguistic and Philosophical Studies, Università Telematica Pegaso, 80132 Napoli, Italy
[e] Department of Chemistry, University of Bari Aldo Moro, via Orabona, 4, 70125 Bari, Italy
[f] Interdepartmental Centre SMART, University of Bari Aldo Moro, via Orabona, 4, 70125 Bari, Italy
[g] Department of Earth and Environmental Sciences, University of Milano Bicocca, Piazza della Scienza 1, 20126 Milano, Italy

ARTICLE INFO

Article history:
Received 15 January 2025
Accepted 19 June 2025
Available online 8 July 2025

Keywords:
Ultramarine
Artificial pigment
Lazurite
VIS spectroscopy
Electron microscopy
Raman spectroscopy

ABSTRACT

The history of ultramarine, a vivid blue pigment derived from lapis lazuli, spans thousands of years. During the 16th to 18th centuries the demand for ultramarine remained high, but its production was limited to specific regions and was extremely expensive. It was used sparingly by artists due to its cost, with some opting for cheaper alternatives such as azurite. In the first half of the 19th century, advancements in chemical knowledge allowed the production of artificial ultramarine, which then spread throughout Europe. The identification of natural versus artificial ultramarine has become a challenge. Here we present analytical results signifying that Raimondo di Sangro (Prince of Sansevero) produced artificial ultramarine before the well-known registered invention by Jean Baptiste Guimet. A detailed study of the chemical composition by SEM-EDS and TEM EDS, along with the absence of accessory minerals commonly found in natural pigment and the presence of uncommon phases, revealed the synthetic origin of the pigment found in the blue frame on the high altar in Sansevero Chapel Museum (Naples, Italy). Moreover, the reflectance spectra disclose an uncommon shift in the main band of the pigment, distinguishing it from both natural ultramarine and more recent synthetic versions. Further, a deep comparison with previous literature data also strengthens our experimental evidence. These results open a new perspective about the first production of this artificial blue pigment.

Introduction and research aim

The gold and blue frame that adorn the high relief, a depiction in marble of the Deposition carved by Francesco Celebrano and Paolo Persico in the 1760s over the High Altar in Sansevero Chapel Museum (Naples, Italy), was commissioned by Raimondo di Sangro (1710–1771), the Prince of Sansevero. He inherited the family chapel along with heavy debts but spared no expense in transforming it into a Baroque masterpiece. Originally built in the late 16th century as a private chapel for the Sansevero family, it reached its artistic and symbolic topmost under the patronage of Raimondo. From the 1740s, he commissioned leading artists to renovate and expand it. A polymath, he conducted scientific experiments in his palace's laboratory, including counterfeit material production. However, the year 1751 proved pivotal: his *Lettera Apologetica* was banned, he lost his position at the Royal Chapel of St. Gennaro after replicating the saint's blood miracle, and Charles of Bourbon outlawed his Masonic lodge. Consequently, Raimondo retreated into his chapel to devote himself to experiments and Masonic ideals, enlisting top sculptors to make it a temple of esoteric artistry. The Sansevero Chapel stands as a unique intersection of Baroque art, Enlightenment thought, and esoteric traditions, embodying Naples' rich cultural and intellectual ferment in the 18th century.

A guide of the Naples city dated 1782 recites: "*Surrounding the high relief is a frame of lapis lazuli invented by the Prince Rai-*

* Corresponding author.
E-mail address: gioacchino.tempesta@uniba.it (G. Tempesta).

https://doi.org/10.1016/j.culher.2025.06.013

mondo, who, spending very little money, forged the lapis lazuli so well that it would fool any professor, even after being sawn into very thin strips. In this paste one can clearly see the exact same gold stains as in real lapis lazuli, and it has the same hardness and weight" [1]. This was an expanded edition of the *Nuova guida de' forestieri*, originally published in 1688 by the Bishop of Bisceglie Pompeo Sarnelli. It was one of the most popular guides to Naples at the time, so influential that the Marquis de Sade used it during his visit to the city in the 1770s. The description of the use of lapis lazuli invented by Raimondo led to an initial characterization of the pictorial layer on-site using mobile instruments. The analysis confirmed that the blue pigment is ultramarine, probably an artificial one, as described in the guide. According to notary de Maggio's inventory, the lapis lazuli frame had not yet been made in 1771 (i.e., at the time of Raimondo's death), and the stone was to be recreated according to the prince's "recipe" [2]. Clearly, it was made in the years following Raimondo's death, but before 1782 [3]. The significant importance of the results necessitates a deeper understanding of the pigment as well as the ligand used, and the techniques applied to decorate and gild the frame to evaluate any potential repaint. The main question to address is the existence of artificial ultramarine before the known production in 1828 by Jean Baptiste Guimet [4]. Subsequently, in the 1840s, ultramarine was adopted by several European artists and produced by various manufacturers such as Wilhelm Buchner (1842), Julius Curtius (1848), Gustav Georg Stinnes (1852) in Germany, and Jean-Louis-Jules Armet de Lisle (1849) in France [5].

There are claims of artificial ultramarine dating back to the 17th century. Haudicquer de Blancourt in 1697, following an English translation made in 1699, stated: "*That the lapis lazuli may be made by art as fine as good as natural, which is gotten from the mines, we allow, and should freely assign the method for it, if there was a scarcity thereof in France, but since we have it in abundance, it is much better to employ the time working in the usual way, than spend it unprofitably by taking a more tedious method*." The statement refers to methods of manufacture which might have nothing to do with lapis lazuli or lazurite. Around this time, Goethe commented during his travels in Italy (1786- 88) that deposits of artificial lapis-like materials were commonplace: "*I prepared myself for a visit to the stone polishers. They are also showing great skill in handling a molten material, which is a by-product of their lime kilns. Among the calcined lime they find lumps of a sort of glass paste, varying in colour from a very light to a very dark or almost black blue. These, like other materials, are cut into thin slabs and priced according to their purity and brilliance of colour. They can be used as successful substitutes for lapis lazuli in the veneering of altars, tombs or other church ornaments*". Considering that Sicilian sulphur is typically found in the same regions as limestone, it is quite possible that aluminosilicates and sulphur occurred in the kilns and that this material was something like ultramarine. Even at this early-stage ultramarine pigments of sorts were being synthesised, intentionally or not, for sale on the open market. Since this practice appears to have been quite widespread, it is a puzzling why information on such materials was not forthcoming. At a time when lapis lazuli was a valuable commodity, it seems likely that anyone with information on a substitute that might be sold as genuine lazurite would not be quick to publicise its existence. Raimondo could have learned the secret practice to produce ultramarine by Sicilian Jesuits [3].

The artificial ultramarine, similar by structure and chemical composition to lazurite, has an approximate formula $Na_{3-5}Al_3Si_3O_{12}S_{1-2}$ which can vary with the manufacturing conditions, namely with the purity and the different proportion of the ingredients. The formula corresponds to ideal lazurite ($Na_3Ca(Al_3Si_3)O_{12}S$), main mineral of the lapis lazuli rock, that at the time of Raimondo was imported from Afghanistan [6]. The pigment ultramarine, extensively used in Europe throughout the 14th and 15th centuries, was obtained by crushing, grinding and cleaning the raw lapis lazuli to separate the other minerals from lazurite. The most famous traditional method to purify lazurite is reported in Cennino Cennini's "*Il Libro dell'Arte*" [7]. The discrimination between natural and artificial ultramarine is not straightforward due to similar chemical composition and properties and usually necessitates of a multi-methodological approach. Generally, lazurite can be recognized with optical microscopy or scanning electron microscopy: the morphology of the pigment particles and variation in the particle size distribution of lazurite are distinctly different from the uniform, small and round particles of the synthetic ultramarine, blue pigment [8]. Also, the presence of associated minerals like pyrite, calcite, diopside, albite, wollastonite, sodalite, forsterite, quartz, phlogopite and others, coexisting in lapis lazuli, can provide a good discrimination between the natural and artificial one.

The development of artificial ultramarine providing a cost-effective and eagerly available alternative to the natural, establishes a significant advance in the pigment industry. The synthetic process involves heating at high temperatures a mixture of sodium carbonate, sulphur, and kaolin, which facilitates the formation of the sodalite structure, which in turn contributes to the vibrant colour associated with ultramarine [9]. Over the years, various refinements in synthesis methods have led to some variations in the chemical composition of artificial ultramarine [10–12,5]. For example, the proportion of sodium to aluminium can slightly vary depending on the manufacturing conditions [5]. Researchers investigate the use of zeolites or waste to enhance pigment stability and environmental sustainability, potentially impacting the final composition [13,11]. The modern synthesis methods had led to the generation of ultramarine variants in different shades, including blue, green, and violet, by altering the synthesis conditions and material inputs [14]. In addition to changes in the base formula, the impurity profiles of synthetic ultramarines have also evolved, as modern synthesis methods allow for better control of contamination and by-product formation [8].

Therefore, chemical data can distinguish natural from artificial ultramarine [8,15,16]. The spectroscopic feature in Raman/luminescence spectra or reflectance spectrum in UV–VIS region or the weak absorption feature in FTIR spectra, can be effective for discrimination [15,17,18]. However, all these studies are referred to artificial ultramarine by nowadays industrial production. Here we employed a multi analytical approach to identify the first artificial ultramarine likely related to an unknown synthesis process of lazurite. We proceeded from the macro to the nanoscale, acquiring both chemical and structural data. We employed fiber optic reflectance (FORS) and Raman spectroscopy; scanning (SEM) and transmission electron microscopy (TEM), both coupled with energy dispersive X-Ray spectroscopy (EDS). Organic ligands were analysed by matrix assisted laser desorption ionization – time of flight – mass spectrometry (MALDI ToF-MS) and reversed phase liquid chromatography – electrospray ionization (RPLC-ESI) – tandem MS.

The data obtained allowed the characterization of this unique ultramarine pigment used in the Sansevero Chapel Museum in Naples with the aim to confirm the historical documents related to the synthetic ultramarine pigment created by Raimondo di Sangro (Prince of Sansevero). The identification and discrimination between natural (hence forth referred to as lapis lazuli) and the synthetic ultramarine is relevant to the analysis of works of art, providing information regarding both the technique used by artists during execution and the historical practice.

Materials and methods

Pictorial layer and reference samples

One fragment of a complete pictorial layer, with traces of the wood support on the bottom, has been detached from the frame (S1-S2). The fragment has been embedded in epoxy resin in a small cylinder and then polished without the use of water or solvents by aluminium oxide abrasive sheets, following steps of decreasing grain size from 30 µm to 3 µm. The prepared surface has been glued to a glassy slide to prepare a 30 μm thick, double polished (repeating the same polishing procedure above) thin section. The thin section has been studied by optical microscopy and then by SEM-EDS. The preparation preserves the morphological integrity of the paint layers, while achieving a high-quality surface suitable for imaging and inorganic mapping studies. The reference samples for spectroscopic measurements and chemical analyses were all obtained from the Department of Earth and Geoenvironmental Sciences at the University of Bari. The natural samples from historical collections were lazurite from Badagshan-Afghanistan (#11349/13) labelled LB and Lazurite from Ariccia-Italy (#10644/2) labelled LA. The spectroscopic measurements were also acquired on one artificial sample of ultramarine pigment from Kremer Pigmente GmbH & Co. KG (#45000) labelled AU.

Optical microscopy (OM)

Cross sections images were acquired by Zeiss Axioskop 40 Pol working in reflected and transmitted light and equipped with a trinocular head connected to a DS-5Mc-U1 digital photomicrographic camera system. A 100 W halogen lamp provided the light source for reflected and transmitted light observations, while a fluorescence illumination system (X-Cite 120) was used to acquire fluorescence images. EC Epiplan-Neofluars Pol objectives with magnifications of 2.5X, 10X, 20X and 50X were used for the study.

Fiber optic reflectance spectroscopy (FORS)

FORS analysis was carried out with a customized system by Avantes. The AvaSpec-ULS2048XL-USB2 spectrophotometer and an AvaLight-HAL-S tungsten halogen light source were combined with a reflection probe FCR-7UV200–2-ME UV/VIS. The spectrophotometer works from 200 to 1100 nm with a spectral resolution of about 1.4 nm. The spectra were recorded from 300 to 800 nm to avoid noise in the UV and IR regions. Diffuse reflectance spectra of the samples were referenced against the WS-2 reference tile, guaranteed to be reflective at 98 % or more in the spectral range investigated. The FORS spectra of all the painted replicas were acquired on the parchment with a spot size diameter of about 2 mm. In all measurements, the distance between the probe and the sample was fixed (~5 mm); for each spectrum, the integration time was 400 ms for 10 scans, for a total acquisition time of 4 s per spectrum. The spectra were collected with Avasoft 8.0 and then exported in Spectragryph® for visualization and comparison with reference standards.

Micro-Raman spectroscopy

A micro-Raman system (BWTEK inc., USA), equipped with a Laser (CleanLaze^{TM}) 785 nm and optical fibres was used. Its tuneable laser power guaranteed the safety of the pictorial layer, while the frequency calibration was performed against the Raman peak of silicon. The instrument was equipped with an optic head with 80X objective, necessary to perform measurements on single grains of the pictorial layer in the thin section. The spectrometer has a spectral resolution of 8 cm^{-1}. Acquisitions were performed with the BWspec 4.03 software, while the data elaboration and the identification of the analysed phases were performed with GRAMS/AI 8.0 suite (Thermo).

Scanning electron microscopy (SEM)

The SEM investigation was made on the thin section coated with a 30-nm-thick carbon film. A SEM EVO-50XVP (Zeiss, Cambridge, UK)), equipped with an Oxford Instruments AZTEC EDS microanalysis system with SD X-Max detector (80 mm^2), was used. Quantitative analyses were obtained though reference standards produced by Micro-Analysis Consultants Ltd. (St. Ives, UK) and X-ray intensities were converted to element by the XPP correction scheme developed by [19,20], implemented in the software by Oxford-Link Analytical (Bicester, Oxfordshire, UK). The operating voltage was 15 kV and the beam current between 150 and 200 pA. Spectra acquisitions lasted 50 s and the working distance was 8.5 mm. Chemical maps were acquired with a counting time of 10 min, and a resolution of 4096 (width) 3328 (height) pixels.

Transmission electron microscopy (TEM)

The TEM investigation was performed at the Platform of Microscopy of the University of Milano-Bicocca (PMiB) with a JEM 2100P (JEOL, Japan) microscope. The instrument is equipped with a LaB_6 source, a Gatan Rio 9 Mpx CMOS camera for image acquisition and an Oxford UltimMax 80 mm^2 SDD detector for EDS analysis. TEM samples were prepared by grazing with a needle, under the stereomicroscope, a small amount of blue pigment from the polished thin section, previously used for optical microscopy and SEM-EDS investigations, then depositing the pigment on a gold grid supporting a holey carbon film, were a droplet (~2 µL) of isopropyl alcohol was preventively deposited. Chemical compositions were quantified with the Cliff and Lorimer approximation [21] using natural standards, as detailed in [22].

Matrix assisted laser desorption ionization – time of flight – mass spectrometry (MALDI ToF-MS)

A 5800 MALDI-ToF/ToF analyzer (AB SCIEX, Darmstadt, Germany) with 10 ppm mass accuracy equipped with a neodymium-doped yttrium lithium fluoride (Nd:YLF) laser (345 nm) was employed in reflectron positive mode for the analysis of the painting binder. Three μL of peptides digest were mixed 1:1 (v:v) with matrix α-Cyano-4-chlorocinnamic acid (CClCA) 10 mg/mL in 70:30 acetonitrile: water (ACN:H_2O) and 0.1 % formic acid (FA) after ZipTip® desalting. One μL of the mixture was applied on MALDI target plate and dried at room temperature. The external calibration was performed using a mixture composed of renin, angiotensin I and ACTH, in the range 800–4000 m/*z*. Usually 1000 laser shots were acquired at laser pulse rates of 400 Hz and each mass spectrum was averaged on at least 6000 shots. The delayed extraction time was set at 240 ns. The peptide mass fingerprint was interpreted with the software Protein prospector (Regents of the University of California) by employing the MS-Fit tool. The acquired MS/MS data set was processed by mMass^{TM} 5.5.0 using MASCOT search engine (Matrix Science, London, United Kingdom), as well as Protein Prospector MS-Tag. The online software BLAST (https://blast.ncbi.nlm.nih.gov/Blast.cgi?PROGRAM=blastp&PAGE_TYPE=BlastSearch&LINK_LOC=blasthome) was also employed to compare the protein sequences and search for similarities with other taxonomies.

Reversed phase liquid chromatography – electrospray ionization (RPLC-ESI) – tandem MS

Liquid chromatographic analyses with tandem MS experiments were performed using an Ultimate 3000 UHPLC coupled with HESI

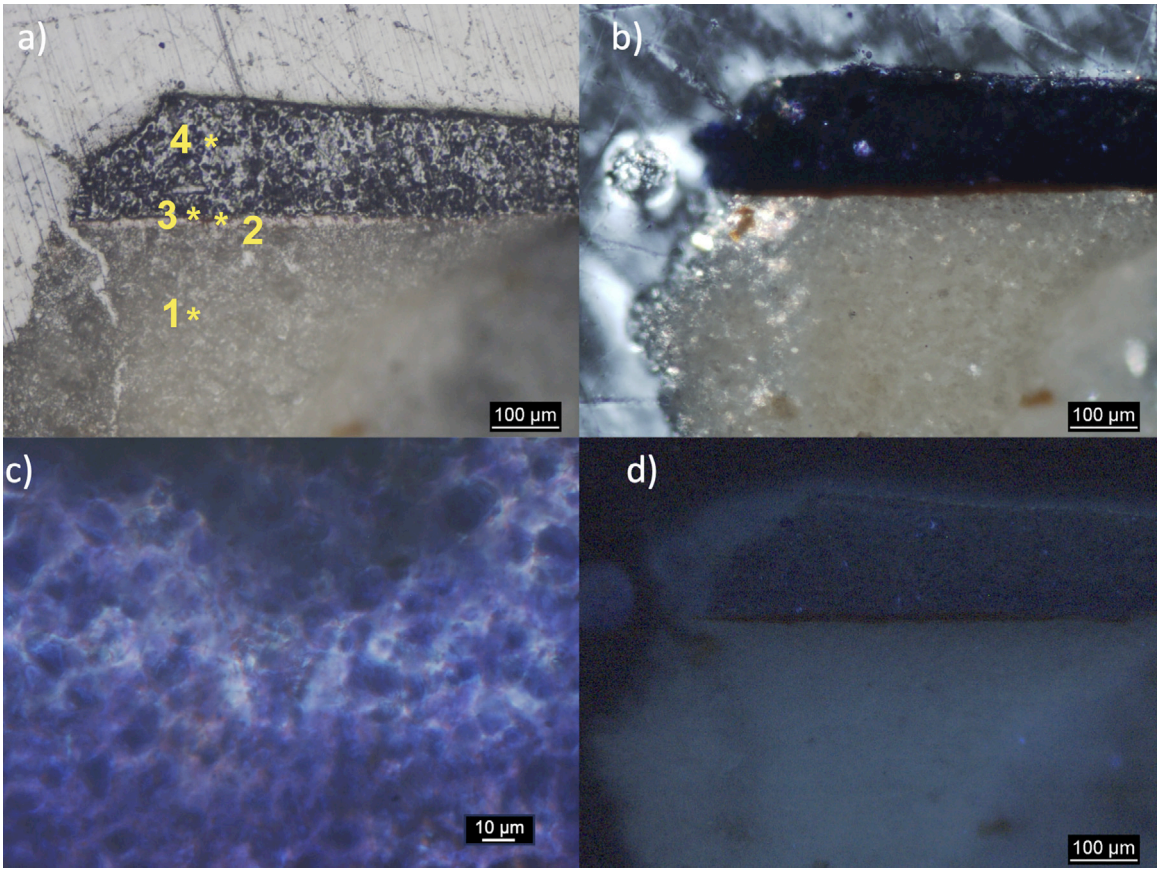

Fig. 1. a) Visible light image of the cross-section (1: ground white layer; 2: red bole layer; 3: gold leaf; 4: pictorial layer); b) crossed polars image show the anomalous birefringence of the epoxy resin; c) enlarged detail of pigment grains; d) in UV light image only the ground layer shows a weak fluorescence.

(heated electrospray ionization) interface and a VelosPro mass spectrometer (Thermo Scientific, Waltham, MA, USA) equipped with a double linear trap mass analyzer. Before the analyses, the purified samples were dried under nitrogen and redissolved into 10 μL 95:5 H_2O:ACN added with 0.1 % FA (v:v). The employed column was an Ascentis® Express C18 (150 mm x 2.1 mm ID, 2.7 μm) equipped with a guard column Ascentis® Express C18 (5 mm x 2.1 mm ID) (Supelco, Sigma-Aldrich Chemie GmbH, Germany) and set at 40 °C. The chromatographic separation was performed at 0.2 mL/min flow with mobile phases H_2O (A) and ACN (B) both with 0.1 % FA using the following gradient: min 0–2 5 % isocratic B; min 2–30 from 5 % to 60 % B; min 30–32 from 60 % to 100 % B; min 32–36 100 % B; min 36–40 from 100 % to 5 % B; min 40–44 re-equilibration to 5 % B. For MS acquisitions, parameters were: sheath gas flow rate 35 a.u. (arbitrary units); spray voltage 3.5 kV; capillary temperature 320 °C; S-Lens RF 60 a.u. Acquisitions were performed in positive ion mode within the *m/z* interval 300–2000 and collisional induced ionization (CID) energy set at 35 % a.u. for MS/MS analysis. The software Xcalibur 2.2 SP1.48 (Thermo Scientific) was used for raw data acquisition, while mMass 5.5.0.0. for spectra elaboration and peak lists extraction.

Results

Optical microscopy (OM)

OM examinations of the cross-section (Fig. 1a) revealed, from top to bottom, a succession of layers: a blue pictorial layer (pl), generally <80 µm thick; an uncommon and expensive *imprimitura* made of a few µm thick gold leaf (gl) (as identified by SEM-EDS, paragraph 3.4.) applied over a preparatory red *bole* layer (rb) (~10 µm thick); and, finally, a thick ground white layer (wl) (~1 mm thick). The red bole layer is typically used for adhering the gold leaf to a wooden surface [23,24]. In this artefact, the gold leaf presence beneath the blue pictorial layer appears unusual, suggesting a unique technique or process. The homogeneity of the layer in the cross-section confirms that the pictorial layer was the untouched original one. No over paintings were observed. The gold leaf was valued for its luminosity, symbolism, and association with wealth and divine light. It was often applied directly onto prepared surfaces, such as wood panels or canvases, and then incorporated into the overall composition of the artwork of religious heritage between the 14th and 18th centuries [24]. The pigment grain size is inhomogeneous, varying from 4 µm to 15 µm (Fig. 1c). The optical images revealed a low refractive index, non-birefringent nature of the pigment, and the absence of strongly birefringent colourless calcite crystals (a characteristic feature of the natural mineral). Additionally, the grains appeared dark under crossed polars (Fig. 1b). The observation under UV shows a light fluorescence from the ground layer and from a thin layer on the surface (Fig. 1d). Some residues of wood support recognisable as a brown layer below gypsum are clearly present (S1).

Fiber optic reflectance spectroscopy (FORS)

The reflectance spectra obtained directly in several point on the frame show common features (S2). A representative spectrum has been compared with those from reference of natural and synthetic ultramarine (Fig. 2). All the spectra normalized show an absorption broad band with minimum around 600 nm. This band, attributed to the S_3^- radical trapped in the structural sodalite cages of lazurite [25] is strictly related to the blue intense colour. The synthetic

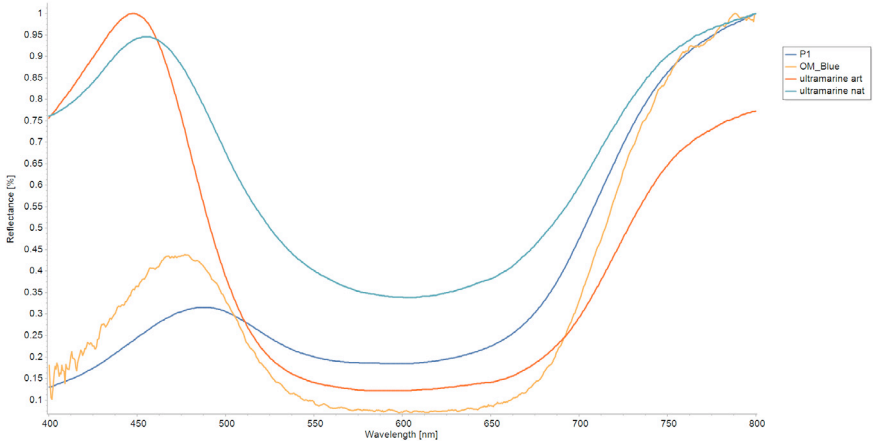

Fig. 2. Reflectance spectra measured on the frame P1(blue) compared with reference of natural ultramarine LB (green) and artificial ultramarine AU (red) and spectrum acquired by optical microscope (orange). All spectra have been normalized.

ultramarine reference shows a most intense absorption with minimum reflectance values, whereas in natural pigments there is an important increase of reflectance. There are also changes in the maximum reflectance band commonly positioned around 450 nm [17,26,27]. The acquired data obtained directly on the frame (P1) show a clear difference compared to references, firstly about the absorption broad band at ~600 nm and secondly regarding the maximum reflectance measured at ~490 nm. The causes could be addressed to the binder, to the gold background or to a mixing with other pigments as already pointed out by [17]. To clarify these aspects, a micro spot in a homogeneous area of the blue pigment was acquired directly with the microscope on the thin section to avoid the gold support contribution (Fig. 1d). The spectrum obtained in this condition, from the pigment and binder, shows a shifted position of the maximum reflectance at ~470 nm. This value is still different from actual artificial ultramarine and natural ultramarine.

Micro-Raman spectroscopy

Raman measurements were easily performed on the prepared cross sections on several grains in the pictorial layer and on the white ground. All grains showed the same spectrum even if affected by fluorescence due to the organic binder. All of them exhibit the characteristic Raman fingerprint of lazurite, which is dominated by the band located at ~548 cm^{-1} assigned to the symmetric stretching vibration (ν_1) of S_3^- radicals. The asymmetry of the main peak at ~548 cm^{-1} could be ascribed to asymmetric stretching (ν_3) of S_3^- at ~580 cm^{-1} or to bending vibrations (ν_4) of SO_4^{2-}. The Raman spectrum acquired with laser at 785 nm on the pictorial layer was compared with spectrum of natural lazurite sample from Afghanistan LB (Fig. 3) and the comparison clearly show a strong luminescence band at ~1300 cm^{-1}.

Scanning electron microscopy (SEM-EDS)

The grain morphology and distribution in the pictorial layer cross-section has been studied by Backscattered Electrons (BSE) SEM images (Fig. 4). Moreover, EDS elemental mapping allowed to distinguish very clearly the regular stratification of the ground layer, the gold thin layer and bole, all below the pictorial layer. The chemical distribution of the main elements (Al, Fe, Au, Ca, S, Si and Na), confirms the stratification described by OM. The cross-section reveals a sequence of layers: a single thick pictorial layer (up to 80 μm thick) over the gold foil (1–2 µm thick), in turn over the Fe-silica rich bole (up to 12 μm thick), over a mix of gypsum and organic matter of the ground. The pictorial layer is homogenous, made only of grains of ultramarine, except few grains of Al (probably a residue of the corundum abrasive used for polishing). In one area of the pictorial layer, one anomalous very small tabular clast (28–12 µm) of barium sulphate (O = 24.27 ± 0.03 wt %; S = 14.42 ± 0.05 wt %; Sr = 2.39 ± 0.08 wt %; Ba = 58.94 ± 0.06 wt %), probably barite, has been observed (Fig. 5). Tens of grains in the pictorial layer with average diameter from 1 µm to 10 µm have been analysed and they all have a composition like lazurite, showing a very low standard deviation for all the main elements (Table 1). The average composition based on 26 negative charges, assuming all sulphur as S^{2-}, in accordance with the standard lazurite formula ($Na_3Ca(Al_3Si_3)O_{12}S$) given in the IMA (International Mineralogical Association) list of minerals, reads: $(Na_{2.67}K_{0.21}Ca_{0.01}Mg_{0.01})_{\Sigma=2.88}(Al_{2.77}Si_{3.07})_{\Sigma=5.84}O_{11.75}(S_{1.22}Cl_{0.06})_{\Sigma=1.28}$. In comparison with the lazurite formula, this composition shows a significant deficiency of extra framework cations (2.88 vs. 4.00), a small deficiency of framework cations (5.84 vs. 6.00), with a slight prevalence of Si over Al (3.07 vs. 2.77), and a slight excess of S (1.28 vs. 1.00). Moreover, sulphur atoms are known to be present in the structure of lazurite in the form of radical ions, such as $(S_2)^-$ and $(S_3)^-$ and SO_4^{2-} [14,28], as confirmed also by Raman. No accessory minerals commonly accompanying lapis lazuli were identified. The gold foil is an alloy of Au (92.23–94.32 wt %) with traces of Ag (3.79–4.96 wt %) and Cu (1.89–2.82 wt %). The bolo layer recalls the composition of a clay with high content of Fe. The ground made of $CaSO_4$ and glue shows a texture of small, variously oriented gypsum crystals, from 3 to 10 µm in length, generally <1 µm thick.

Transmission electron microscopy (TEM-EDS)

Among the several tens of crystals examined, the majority has a chemical content compatible with lazurite, i.e. S-bearing Na-aluminosilicate, ± Ca, ± K, ± Cl. For some of these crystals, along with the EDS spectrum it was possible to collect a selected area electron diffraction (SAED) pattern along a main zone axis and therefore to identify them as lazurite thoroughly (Fig. 6 and S3). The structure taken as reference was the Sary-Sang (Afghanistan) lazurite determined by [29] in the *P*-43*n* space group, with a = 9.105 Å. Generally, the lazurite crystals have dimensions spanning from few hundred of nm to few microns. The chemical compositions determined for the four indexed crystals by TEM-EDS analysis are reported in Table 2. The average chemical composition of the studied crystals recalculated on the basis of 26 negative charges reads:

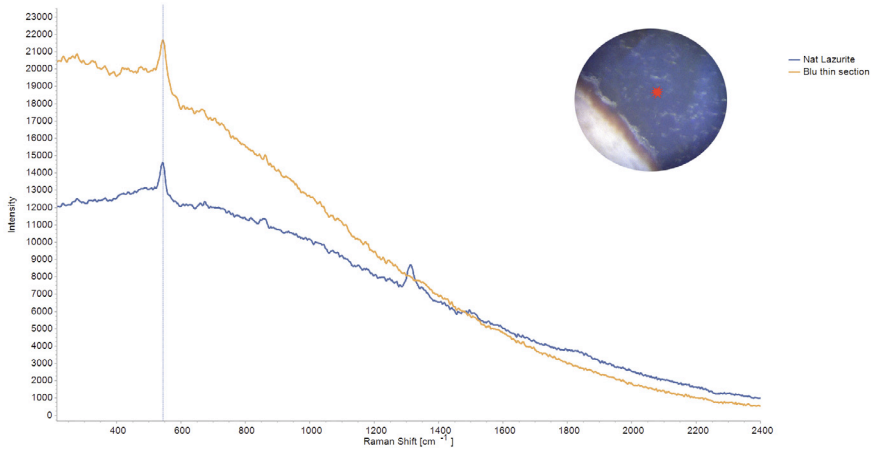

Fig. 3. Raman spectrum executed on a grain of a blue pigment (picture in the box upper right) in orange, compared with spectrum of natural lazurite in blue from Afghanistan LB.

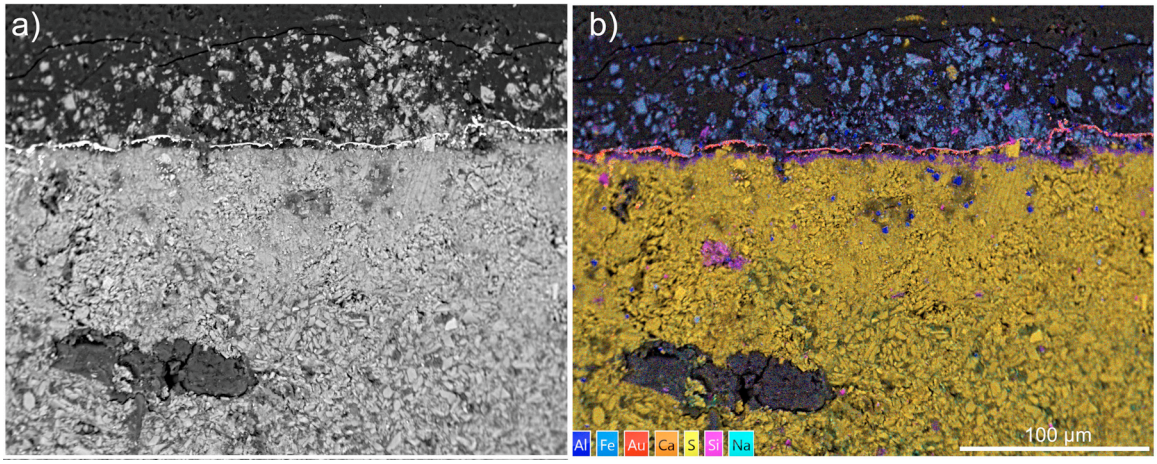

Fig. 4. SEM micrograph in BSE mode of the cross-section (a) and associated elemental layered map of Al, Fe, Au, Ca, S, Si and Na (b).

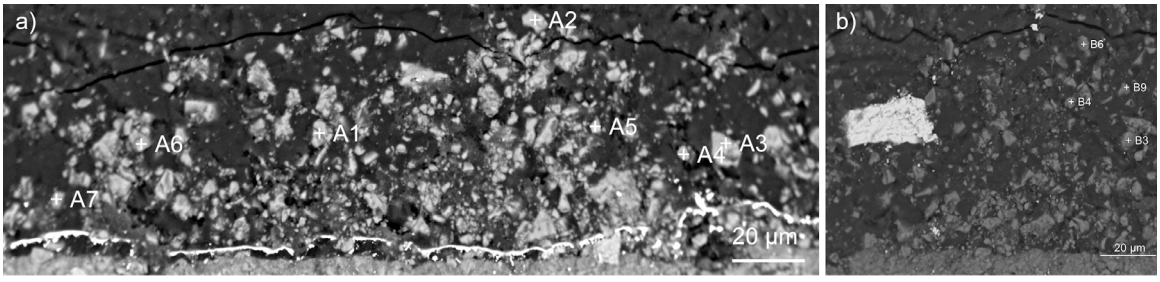

Fig. 5. SEM-BSE images showing (a) the pictorial layer with indication of the EDS spot analyses (A) and (b) a large bright crystal of barium sulphate and indication of EDS spot analyses (B).

Table 1
Semi-quantitative SEM-EDS analysis of 13 deep blue particles in the pictorial layer ascribed to lazurite-like phase, recalculated on the basis of 26 negative charges (A.p.f.u. = Atom per formula unit).

A.p.f.u.	A 1	A 2	A 3	A 4	A 5	A 6	A 7	B2	B3	B4	B6	B9	Mean	StDev
O	11.79	11.73	11.72	11.78	11.81	11.70	11.78	11.66	11.76	11.77	11.66	11.83	**11.75**	**0.06**
Na	2.70	2.49	2.55	2.68	2.69	2.49	2.54	2.48	2.94	2.70	2.66	3.14	**2.67**	**0.20**
Mg	0.00	0.05	0.04	0.00	0.00	0.00	0.03	0.00	0.00	0.00	0.00	0.00	**0.01**	**0.02**
Al	2.75	2.73	2.69	2.84	2.82	2.63	2.79	2.77	2.75	2.78	2.83	2.84	**2.77**	**0.06**
Si	3.06	3.13	3.13	3.04	3.08	3.19	3.11	3.07	3.03	3.05	2.98	2.97	**3.07**	**0.06**
S	1.22	1.22	1.24	1.17	1.16	1.25	1.19	1.32	1.22	1.20	1.33	1.15	**1.22**	**0.06**
Cl	0.00	0.09	0.08	0.10	0.07	0.08	0.05	0.03	0.05	0.05	0.02	0.05	**0.06**	**0.03**
K	0.26	0.19	0.20	0.20	0.16	0.23	0.19	0.22	0.22	0.24	0.25	0.13	**0.21**	**0.04**
Ca	0.06	0.00	0.00	0.00	0.00	0.00	0.00	0.00	0.00	0.02	0.00	0.00	**0.01**	**0.02**
Σ_T	5.81	5.86	5.83	5.88	5.89	5.82	5.89	5.84	5.78	5.84	5.81	5.80	**5.84**	**0.04**
Σ_A	3.02	2.72	2.79	2.88	2.85	2.72	2.76	2.70	3.16	2.96	2.91	3.27	**2.90**	**0.18**

Σ_T = tetrahedral cations; Σ_A = all the other cations.

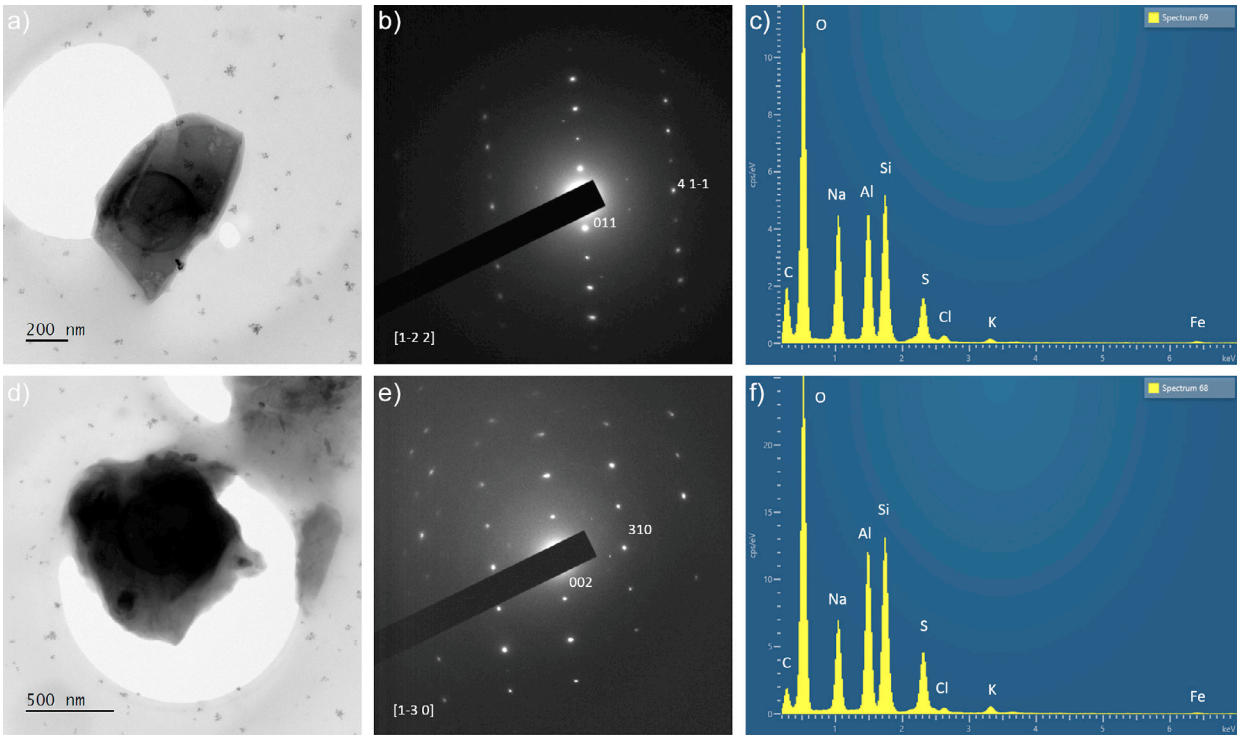

Fig. 6. Bright field TEM images (a, d), selected area electron diffraction (SAED) patterns (b, d) and EDS spectra (c, f) of representative lazurite crystals found in the blue pigment. Main reflections are indicated (in white) on the SAEDs, as well as the electron beam incidence (in square brackets).

Table 2
Semi-quantitative TEM-EDS analysis of lazurite crystals found in the blue pigment recalculated on the basis of 26 negative charges.

A.p.f.u.	1	2	3	4	Mean	St. Dev.
O	11.91	12.28	11.83	11.92	**11.99**	**0.20**
Na	2.63	2.40	2.01	3.22	**2.57**	**0.51**
Mg	0.02	0.04	0.00	0.00	**0.01**	**0.02**
Al	2.89	2.98	3.00	2.76	**2.91**	**0.11**
Si	3.02	3.15	3.11	3.04	**3.08**	**0.06**
P	0.03	0.00	0.00	0.00	**0.01**	**0.02**
S	1.06	0.70	1.13	1.01	**0.98**	**0.19**
Cl	0.06	0.03	0.08	0.14	**0.08**	**0.04**
K	0.11	0.41	0.12	0.08	**0.18**	**0.15**
Ca	0.01	0.00	0.01	0.02	**0.01**	**0.01**
Σ_T	5.91	6.13	6.12	5.80	**5.99**	**0.16**
Σ_A	2.80	2.85	2.14	3.32	**2.78**	**0.48**

Σ_T = tetrahedral cations; Σ_A = all the other cations.

$(Na_{2.57}K_{0.18}Ca_{0.01}Mg_{0.01})_{\Sigma=2.78}(Al_{2.91}Si_{3.08})_{\Sigma=5.99}O_{11.99}(S_{0.98}Cl_{0.08})_{\Sigma=1.06}$. This TEM-EDS average composition compares very well with the average composition obtained by SEM-EDS and, as for the latter, in comparison to ideal lazurite, it shows a slight prevalence of Si over Al and a significant deficiency of extra framework cations, such as Na and K, and is practically free of Ca. Since this same trend was observed with two independent techniques, we believe it could be real and could represent a signature of the artificial nature of the pigment. Other than lazurite-like grains, we also detected some minor Sn-bearing silicates and Ba-bearing grains (Fig. S4).

Matrix assisted laser desorption ionization – time of flight – mass spectrometry (MALDI ToF-MS) and reversed phase liquid chromatography – electrospray ionization (RPLC-ESI) – tandem MS

A tiny fragment of the sample was used to perform micro-destructive analysis to investigate the organic fraction. Fig. 7 shows the MALDI-MS peptide mass fingerprinting (PMF). Mass signals in the spectrum can be attributed to the typical tryptic and chymotryptic digestion pattern of an animal glue, particularly mammal, according to the results obtained from previous studies in scientific literature [30–34] and the ones provided by the bioinformatic search via Protein Prospector. By following a typical bottom-up proteomic approach, RPLC-ESI-MS/MS experiments were performed to clearly assess the primary structure of the peptides composing the binder in the painting layer. Some examples are shown in Figure S5 where the fragmentation of the double-charged ions at *m/z* 449.8 (panel A), *m/z* 730.4 (panel B) and *m/z* 824.9 (panel C), respectively corresponding to (R)GVVGLP(Oxidation)GQR(G), (R)GSAGPP(Oxidation)GATGFP(Oxidation)GAAGR(V) both from collagen $\alpha-1$(I) and (R)GSTGEIGPAGPP(Oxidation)GPP(Oxidation)GLR(G) from collagen $\alpha-2$(I) chain, are reported. Regarding taxonomy, we found out that most of the investigated peptides were attributable to *Bos taurus* collagen thus suggesting the use of a glue based on bovine tissue. Despite some sequences have shown a 100 % identity in BLAST with other taxonomies like sheep, pig or goat, the software confirmed that all the sequenced peptides belong to bovine collagen. Anyway, three ions represented an exception, i.e. *m/z* 1180.6, 1196.6 and 1162.6 (Fig. 7), as they were identified respectively as (R)TGQPGAVGPAGIR(G), (R)TGQPGAVGPAGIR(G) + 1 oxidation (from Fibrillar collagen NC1 domain, *Ovis aries*) and (T)VNQGNPYLEK(D) + 1 deamidation (collagen $\alpha-1$(XVII) chain, *gallus*). Indeed, ions at *m/z* 1180.6 and 1196.6 have already been reported as marker peptides for sheep according to previous collagen speciation studies [35,36]. The MS^2 spectra of two of these ions are reported in Figure S6. These findings support the hypotheses that a mix of different animal species is present in the glue employed for the investigated painting layer. However, we cannot rule out that the same glue was employed for preparatory red *bole* layer or ground white layer since the whole fragment has been subjected to in-solution tryptic digestion.

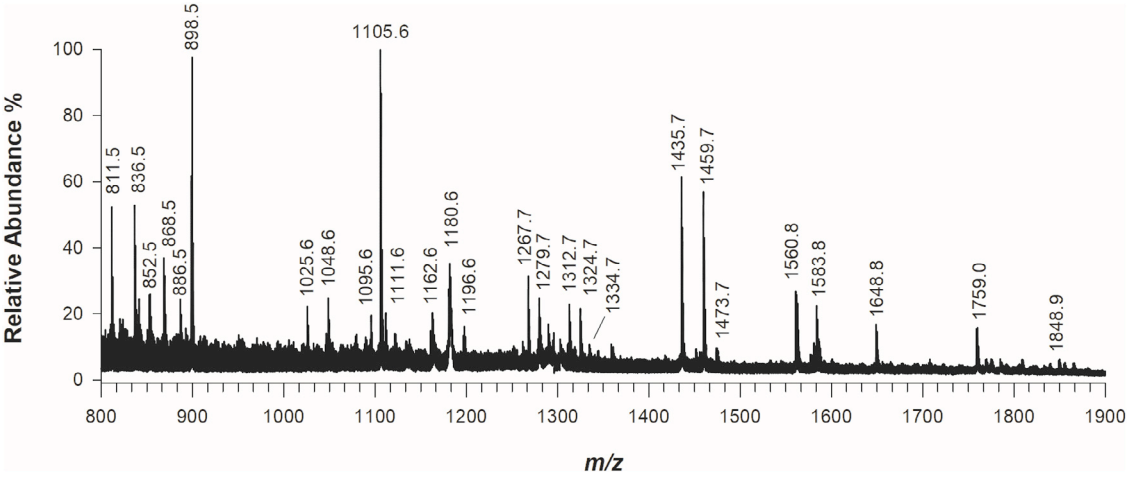

Fig. 7. MALDI Peptide mass fingerprinting (PMF) of a blue layer painting sample collected from Cappella Sansevero, Napoli, Italy, revealing the presence of animal collagen as binder.

Discussion

The organic binder analyses confirm the presence of animal collagen used as glue for both ground and pigment layer. This is fully in agreement with the techniques used in 18th century for the ground preparation and not very common for pictorial layers [24]. Indeed, the use of collagen-based tempera paint has been widespread in Italy at least until the 16th century [6,37] and it was especially appreciated for the brightness conferred to the polychromies [38]. Animal glues were obtained by boiling tissues such as bones, skin, and cartilage of mainly rabbits or bovines, or from fish swim bladder [31,39] and then employed as painting media. Furthermore, the OM observations confirm the presence of a single blue layer (thick <80 µm). The pigment's grain morphology and their size (4.0 to 15 µm), observed with OM and SEM-BSE images (Figg.1d, 4 and 5), are similar to those observed in natural ultramarine pigments, which usually are of less homogeneous appearance, contrary to the artificial pigment, commonly described as rounded particles of regular size (0.5 to 5.0 µm) and shape [6]. In any case, no other mineralogical phases, such as pyrite, calcite, diopside, albite, wollastonite, sodalite, forsterite, quartz, phlogopite etc., commonly found in natural ultramarine, were identified by OM, µRaman, SEM-EDS and TEM-EDS. All the µRaman spectra acquired with 785 nm laser source exhibit the same characteristic fingerprint of lazurite. The spectra do not show the typical strong luminescence signal at 1300 cm^{-1} that distinguish natural lazurite from Afghanistan from artificial lazurite [18]. All the FORS spectra acquired onsite directly onto the frame (Fig. S2), show a red shift to 490 nm of the maximum reflectance band, significantly different from the 450 nm shift commonly found in artificial ultramarine, rising some doubts about the purity of the pigment [17]. The hypothesis of a mix of pigments was excluded by OM and SEM results. So, to evaluate the influence of the gold ground on the spectra acquired on the frame, reflectance measurements were acquired directly on the ultramarine grains at the microscope. The results confirm the red shift of ~ 20 nm, validating the idea that the gold substrate affects the measure. Anyhow, the characteristic main reflectance band at ~470 nm for artificial ultramarine has never been reported in the literature for a pure pigment, which therefore arises as a distinguish feature of this artificial ultramarine. The chemical data obtained by SEM-EDS of all blue grains analysed in thin sections are very similar and different from those measured on natural grains of ultramarine pigment. A comparison of normalized SEM-EDS data (wt %) of the major and minor elements measured on 13 blue grains with (i) those of natural lazurite from different sources [15], (ii) those from today synthetic grains of ultramarine (Fig. 8), and (iii) one natural lazurite (LA) from Ariccia (Italy), clearly shows the non-natural source of Sansevero Chapel ultramarine.

The main evidence relates on (i) the lack of Ca and (ii) the non-tetrahedral cation composition of the lazurite like grains, generally lower than in natural lazurite. Lazurite, the principal component of lapis lazuli, is a framework silicate belonging to the sodalite group whose structure consists of alternating corner-sharing SiO_4^{4-} and AlO_4^{5-} tetrahedra forming a 3D architecture of interconnected 6-membered and 4-memebered rings. Non-tetrahedral cations such as Na^+ and Ca^{2+}, and occasionally K^+, occupy larger cages at the center of the 6-memebred rings. The arrangement and concentration of non-tetrahedral cations can significantly affect the optical properties of lazurite, influencing its hue and color intensity and stability [40,41]. Ongoing research into the behavior and distribution of these cations enhances the understanding of color generation in lazurite and could lead to advancements in synthetic ultramarine pigments and related applications. In artificial homologues of lazurite, the aluminosilicate framework allows a very wide range of cage cation and anion substitutions, which makes very common to find in early 19th synthesis of "ultramarine" heavy elements such as Ag, Tl, Sr, Ba, Zn, Mn, Pb, and Se in the pigment composition [42]. These heavy elements are easy to recognize in BSE images, whose contrast is sensitive to the average Z-number of the imaged object, but only one Ba-bearing grain was identified by SEM-EDS, an outcome also confirmed by TEM-EDS. Some elements like Si, Cl, and S were chosen as discriminative elements in the provenance study of lazurite [43], connecting their relative proportions to different genetic environments. Therefore, evaluating the range of Al/Si, Cl/Si and S/Si ratios of the natural sample from Afghanistan [15], early artificial ultramarine [9], and the blue pigment studied here, several differences arise (Table 3), adding a robust confirmation of the different, unknown production process invented by Raimondo di Sangro.

To further constrain the origin of the lazurite grains analysed in this study, similarly to Ajò et al. [44], who represented Na/Si ratio vs. Al/Si ratios, we plot our chemical data obtained by SEM-EDS along with those from literature [15,44–47], for both artificial and natural samples (Fig. S7). From this comparison, some superpositions between natural samples and artificial samples are evident, as for instance in the case of Early artificial samples from Wilkens [45] and natural samples from Afghanistan from Favaro et al. [15]. Therefore, to better distinguish natural from artificial samples, we found that plotting Ca/Na vs. Al/Si, instead of the Na/S vs. Al/Si, is

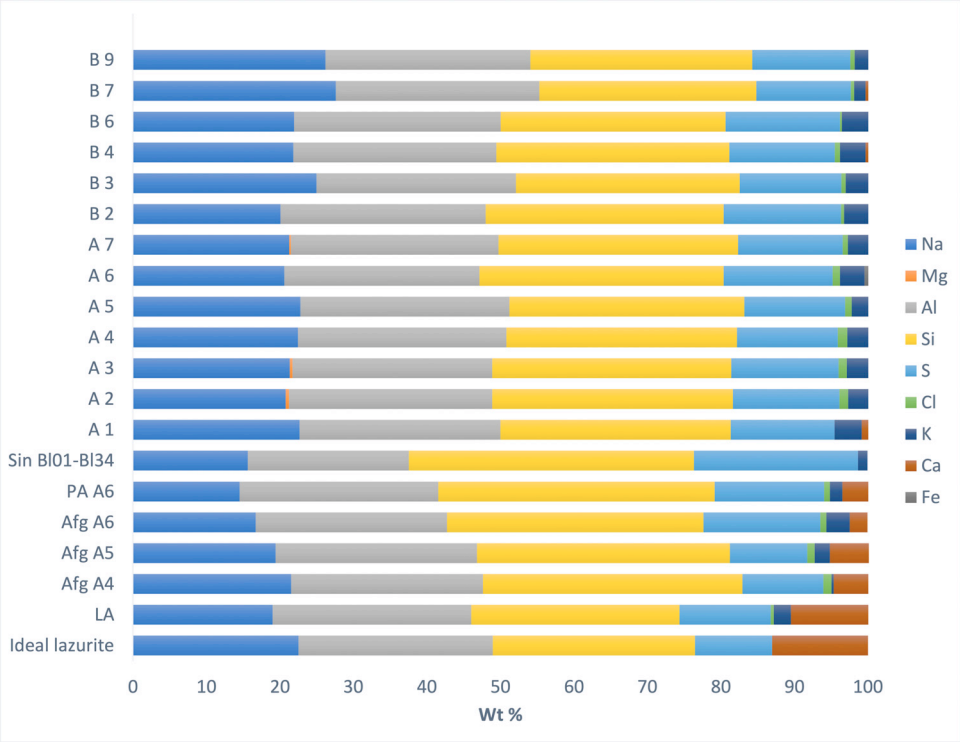

Fig. 8. Bar chart of chemical composition of blue pigment grains from this study (A1 to A7 and B2 to B9) compared with data of natural ultramarine from Afghanistan (Afg A4 to A6, PA6) and average composition of synthetic pigment (Sin B101-B134) from Favaro et al. (2012) vs ideal lazurite and natural lazurite from Campania (Italy) analysed by SEM-EDS (LA).

Table 3
The range of values related to Al/Si, Cl/Si, and S/Si ratios was calculated from SEM-EDS data of the studied pigment (Blue pigment), literature data for Afghanistan ultramarine [15], and early different production of artificial ultramarine (Early art.) [9].

	Blue pigment	Afghanistan	Early artificial			
Ratio	Average	Min - Max	Average	Min - Max	Average	Min - Max
Al/Si	0.88	0.80–0.92	0.75	0.72–0.80	0.77	0.64–0.80
Cl/Si	0.02	0.01–0.04	0.02	0.02–0.03	/	/
S/Si	0.45	0.44–0.51	0.38	0.30–0.40	0.70	0.61–0.77

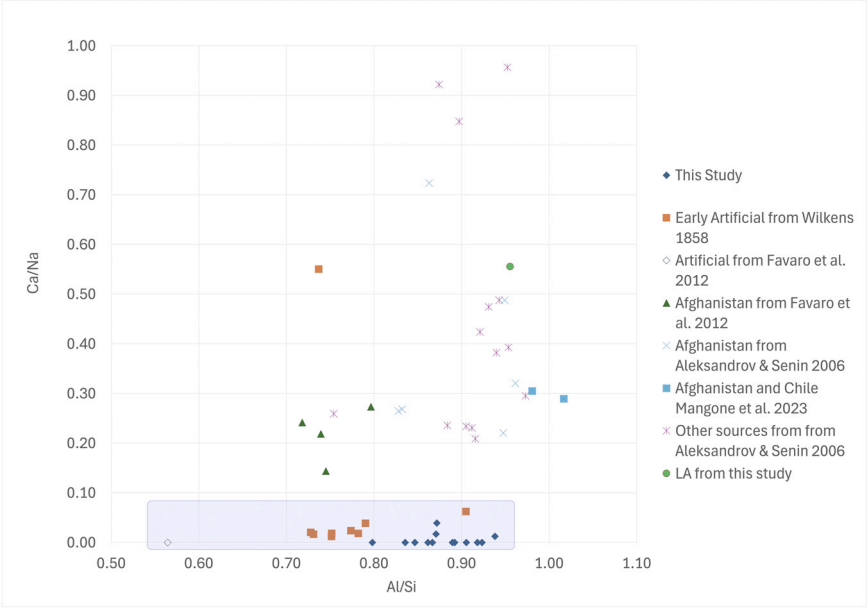

Fig. 9. Distribution of the natural and artificial ultramarine, based on the Ca/Na ratio vs Al/Si ratio.

more effective (Fig. 9). Indeed, Ca and Na in lazurite are vicariant in the same structural site, therefore are more sensitive to growth environment or synthesis conditions than other elements.

Moreover, by TEM-EDS minor Sn-bearing silicates were identified, never reported before in ultramarine analyses. These phases, that do not belong to lapis lazuli, could shed a light on the secret formula known by Raimondo di Sangro for ultramarine making. The exceptional quality of the crystals produced can be inferred by the crystallinity evidenced by SAED patterns and the derived structural parameters that well fit with those of natural lazurite described by Hassan et al. [29].

Conclusions

The very low content or absence of Ca in pigment grains found by SEM-EDS and TEM-EDS, makes this characteristic the main clue for the artificial origin attribution of the pigment together with the absence of the peculiar Raman luminescence. This study seems to confirm the documents describing Raimondo di Sangro's ability to reproduce lapis lazuli. Moreover, the results suggest the need to explore, in the future, the previously unknown production of ultramarine in Sicily, following the earliest description divulged by Goethe. In fact, De Ceglia et al. [3] hypothesized that Raimondo learned the secret practice to produce ultramarine by Sicilian Jesuits. The results of this study push back the date of the first artificial ultramarine invention made by Jean Baptiste Guimet by at least fifty years. This is significant because Klaproth's publication (1797) was the first to identify the presence of sulphur in lapis lazuli. At that time, it was believed that the blue colour of this material resulted from the presence of iron, copper or cobalt. Three years later, Guyton de Morveau (1800) confirmed that the origin of the blue colour involves sulphur. These results suggest that all of those involved in the study of 18th-century works of arts should pay close attention to the origin of ultramarine, when it is present.

Author contributions

G.T., A.M., F.P.C and A.M. designed the study. G.T. and A.M. performed the FORS analyses. G.T prepared the sample in thin section and characterize it by OM, Raman and SEM. G.C. performed TEM analyses. E.C.L.R. and C.D.C executed MALDI-ToF-MS and RPLC-ESI-MS/MS. The manuscript was written by G.T., A.M., C.D.C., E.C.L.R. and G.C. with the comments and input from all co-authors.

Data availability

The datasets used and/or analysed during the current study available from the corresponding author on reasonable request

Acknowledgments

This research was supported by the Italian Ministry of University and Research (mur) grant prin 2017 2017EX5AC3_001 "The uncertain borders of nature. Wonders and miracles in early modern Naples" and by PRIN2022 cod. 2022CNNRWZ "REActive GEl for orgaNic bindERs recognition in Artworks" granted by MUR. We wish to thank Maria Alessandra Masucci, President and Director of the Museo Cappella Sansevero, for her invaluable collaboration. Thanks, are also due to Nicola Mongelli for help in carrying out the Scanning Electron Microscopy (SEM) with Energy Dispersive X-Ray Spectroscopy (EDS) investigations. We sincerely thank the Reviewers, we truly appreciate the time, effort, and expertise devoted to reviewing our work. All comments and suggestions have been invaluable in improving the clarity and quality of the manuscript.

Supplementary materials

Supplementary material associated with this article can be found, in the online version, at doi:10.1016/j.culher.2025.06.013.

References

[1] P. Sarnelli, Nuova guida de' Forestieri, e dell'Istoria di Napoli, con cui si vede, e si spiegano le cose pi˜notabili della medesima, e del suo amenissimo distretto, con una distinta descrizione di tutte l'eruzioni da volta in volta fatte dal Monte Vesuvio, Nuova Edizione Ampliata Delle Molte Moderne Fabbriche Secondo Lo Stato Presente, Ed Arricchita Di Varie Figure, Napoli, 1772.
[2] S. Attanasio, In Casa del Principe di Sansevero. Architettura, Invenzioni, Inventari, Napoli, 2011.
[3] F.P. De Ceglia, A. Maraschi, A. Monno, G. Tempesta, In search of the phoenix in eighteenth-century Naples Raimondo di Sangro, nature mimesis, and the production of counterfeit stones between palingenesis, alchemy, art, and economy, Nuncius 39 (2) (2024) 451–485, doi:10.1163/18253911-bja10097.
[4] J. Mérimée, Rapport sur le prix proposé pour la fabrication d'un outremer artificiel, Bull. Soc. Encourag. pour Ind. Natl. 27 (293) (1828) 346–349.
[5] Mertens Joost, The history of artificial ultramarine (1787-1844): science, industry and secrecy, Ambix 51 (3) (Nov. 2004) 219–244, doi:10.1179/amb.2004.51.3.219.
[6] J. Plesters, "Ultramarine blue, natural and artificial," 1966.
[7] C. Cennini, Il Libro Dell'arte, o Trattato della pittura, Firenze, 1859.
[8] I. Osticioli, N.F.C. Mendes, A. Nevin, F.P.S.C. Gil, M. Becucci, E. Castellucci, Analysis of natural and artificial ultramarine blue pigments using laser induced breakdown and pulsed raman spectroscopy, statistical analysis and light microscopy, Spectrochim Acta Mol Biomol Spectrosc 73 (3) (Aug. 2009) 525–531, doi:10.1016/j.saa.2008.11.028.
[9] H. Wilkens, On artificial ultramarines, J Frankl. Inst 35 (1858) 136–138.
[10] D.G. Booth, "The synthesis and structure of ultramarine pigments," 2001.
[11] Y.H. Hsiao, Y.H. Shen, D.T. Ray, Synthesis of ultramarine from reservoir silts, Minerals 7 (5) (May 2017), doi:10.3390/min7050069.
[12] D. Arieli, D.E.W. Vaughan, D. Goldfarb, New synthesis and insight into the structure of blue ultramarine pigments, J. Am. Chem. Soc. 126 (18) (May 2004) 5776–5788, doi:10.1021/ja0320121.
[13] H. Wang, Z. Zhen, S. Yao, S. Li, Synthesis of high acid-resistant ultramarine blue pigment through coal gangue, industrial zeolite waste and corn straw waste recycling, Resour. Chem. Mater. 1 (2) (Jun. 2022) 137–145, doi:10.1016/j.recm.2022.03.003.
[14] R.J.H. Clark, T.J. Dines, and M. Kurmoo, "On the nature of the sulfur chromophores in ultramarine blue, green, violet, and pink and of the selenium chromophore in ultramarine selenium: characterization of radical anions by electronic and resonance raman spectroscopy and the determination of their excited-State geometries," 1983.
[15] M. Favaro, A. Guastoni, F. Marini, S. Bianchin, A. Gambirasi, Characterization of lapis lazuli and corresponding purified pigments for a provenance study of ultramarine pigments used in works of art, Anal. Bioanal. Chem. 402 (6) (Feb. 2012) 2195–2208, doi:10.1007/s00216-011-5645-4.
[16] A. Pourliaka, L. Malletzidou, T. Zorba, K.M. Paraskevopoulos, E. Pavlidou, and G. Vourlias, "Towards the discrimination between natural and synthetic pigments: the case of ultramarine," in 11th International Conference of the Balkan Physical Union (BPU11) - S06-CMPSP Condensed Matter Physics and Statistical Physics, Belgrade, 2022. [Online]. Available: https://pos.sissa.it/
[17] M. Aceto, A. Agostino, G. Fenoglio, M. Picollo, Non-invasive differentiation between natural and synthetic ultramarine blue pigments by means of 250-900 nm FORS analysis, Anal. Methods 5 (16) (Aug. 2013) 4184–4189, doi:10.1039/c3ay40583d.
[18] M. González-Cabrera, P. Arjonilla, A. Domínguez-Vidal, M.J. Ayora-Cañada, "Natural or synthetic? Simultaneous raman/luminescence hyperspectral microimaging for the fast distinction of ultramarine pigments, Dyes Pigments 178 (Jul. 2020), doi:10.1016/j.dyepig.2020.108349.
[19] J.-L. Pouchou, F. Pichoir, Quantitative analysis of homogeneous or stratified microvolumes applying the model 'pap, in: Electron Probe Quantitation, Springer, 1991, pp. 31–75, doi:10.1007/978-1-4899-2617-3_4.
[20] D.S. COOMBS, Y. NAKAMURA, M. VUAGNAT, Pumpellyite-actinolite facies schists of the Taveyanne Formation near Loèche, J. Petrol. 17 (4) (Nov. 1976) 440–471, doi:10.1093/petrology/17.4.440.
[21] G. Cliff, G.W. Lorimer, The quantitative analysis of thin specimens, J. Microsc. 103 (2) (Mar. 1975) 203–207, doi:10.1111/j.1365-2818.1975.tb03895.x.
[22] R. Conconi, G. Ventruti, F. Nieto, G. Capitani, TEM-EDS microanalysis: comparison among the standardless, Cliff & Lorimer and absorption correction quantification methods, Ultramicroscopy 254 (2023) 113845, doi:10.1016/j.ultramic.2023.113845.
[23] D. Hradil, J. Hradilová, P. Bezdička, C. Serendan, Late Gothic/early Renaissance gilding technology and the traditional poliment material 'Armenian bole': truly red clay, or rather bauxite? Appl. Clay Sci. 135 (2017) 271–281, doi:10.1016/j.clay.2016.10.004.
[24] I.C.A. Sandu, L.U. Afonso, E. Murta, M.H. De Sa, Gilding techniques in religious art between east and west, 14th-18th centuries, Int. J. Conserv. Sci. 1 (1) (2010) 47–62.
[25] D. Reinen and G. Lindner, "The nature of the chalcogen colour centres in ultramarine-type solids," 1990.

[26] G. Tempesta, C. Porfido, M. Bellino, A. Monno, The 'exultet 1' of Bari: multi-methodological approach for the study of a rare medieval parchment roll, Period. Mineral. 87 (2) (2018), doi:10.2451/2018PM753.
[27] S. Farsang, R. Caracas, T.B.M. Adachi, C. Schnyder, Z. Zajacz, S ·3radicals and the S·24polysulfide ion in lazurite, haöyne, and synthetic ultramarine blue revealed by resonance Raman spectroscopy, Am. Mineral. 108 (12) (Dec. 2023) 2234–2243, doi:10.2138/am-2022-8655.
[28] N. Gobeltz-Hautecoeur, A. Demortier, B. Lede, J.P. Lelieur, C. Duhayon, Occupancy of the sodalite cages in the blue ultramarine pigments, Inorg. Chem. 41 (11) (Jun. 2002) 2848–2854, doi:10.1021/ic010822c.
[29] I. Hassan, R.C. Peterson, H.D. Grundy, The structure of lazurite, ideally Na6Ca2(Al6Si6O24)S2, a member of the sodalite group, Acta Crystallogr. C 41 (6) (Jun. 1985) 827–832, doi:10.1107/S0108270185005662.
[30] R. Hynek, S. Kuckova, J. Hradilova, M. Kodicek, Matrix-assisted laser desorption/ionization time-of-flight mass spectrometry as a tool for fast identification of protein binders in color layers of paintings, Rapid Commun. Mass Spectrom. 18 (17) (Sep. 2004) 1896–1900, doi:10.1002/rcm.1570.
[31] S. Dallongeville, N. Garnier, C. Rolando, C. Tokarski, Proteins in art, archaeology, and paleontology: from detection to identification, Chem. Rev. 116 (1) (Jan. 2016) 2–79, doi:10.1021/acs.chemrev.5b00037.
[32] T. Tripković, et al., Identification of protein binders in artworks by MALDI-TOF/TOF tandem mass spectrometry, Talanta 113 (2013) 49–61, doi:10.1016/j.talanta.2013.03.071.
[33] I.D. van der Werf, C.D. Calvano, G. Germinario, T.R.I. Cataldi, L. Sabbatini, Chemical characterization of medieval illuminated parchment scrolls, Microchem. J. 134 (2017) 146–153, doi:10.1016/j.microc.2017.05.018.
[34] C.D. Calvano, E. Rigante, R.A. Picca, T.R.I. Cataldi, L. Sabbatini, An easily transferable protocol for in-situ quasi-non-invasive analysis of protein binders in works of art, Talanta 215 (2020), doi:10.1016/j.talanta.2020.120882.
[35] M. Buckley, M. Collins, J. Thomas-Oates, J.C. Wilson, Species identification by analysis of bone collagen using matrix-assisted laser desorption/ionisation time-of-flight mass spectrometry, Rapid Commun. Mass Spectrom. 23 (23) (Dec. 2009) 3843–3854, doi:10.1002/rcm.4316.
[36] S. Hickinbotham, S. Fiddyment, T.L. Stinson, M.J. Collins, How to get your goat: automated identification of species from MALDI-ToF spectra, Bioinformatics 36 (12) (Jun. 2020) 3719–3725, doi:10.1093/bioinformatics/btaa181.
[37] Leonardo da Vinci, Trattato Della Pittura, Carabba, Lanciano, 1947 [Online]. Available http://www.e-text.it/ .
[38] L. Campanella, et al., Chimica Per L'arte, Zanichelli editore S.p.A, Bologna, 2007 Accessed: Apr. 14, 2025. [Online]. Available: https://www.zanichelli.it/ricerca/prodotti/chimica-per-l-arte .
[39] Maartje.J.N. Stols-Witlox, Historical Recipes for Preparatory Layers for Oil Paintings in Manuals, Manuscripts and Handbooks in North West Europe, 1550-1900: Analysis and Reconstructions, Universiteit van Amsterdam, 2014 [Online]. Available https://api.semanticscholar.org/ CorpusID.
[40] M.C. Caggiani, A. Mangone, P. Acquafredda, Blue coloured haüyne from Mt. Vulture (Italy) volcanic rocks: SEM-EDS and Raman investigation of natural and heated crystals, J. Raman Spectrosc. 53 (5) (May 2022) 956–968, doi:10.1002/jrs.6310.
[41] G.Della Ventura, F. Capitelli, M. Sbroscia, A. Sodo, A Raman study of chalcogen species in sodalite-group minerals from the volcanic rocks of Latium (Italy), J. Raman Spectrosc. 51 (9) (Sep. 2020) 1513–1521, doi:10.1002/jrs.5665.
[42] F.M. Jaeger, Sur les outremers naturels et artificiels, Bull. Soc. fr. Minéral. 53 (1) (1930) 183–209, doi:10.3406/bulmi.1930.4093.
[43] J. Zoeldfoeldi, S. Richter, Z. Kasztovszky, and J. Mihaly, "Where does Lapis Lazuli come from? Non-destructive provenance analysis by PGAA," 34th International Symposium on Archaeometry, 2006-01-01, ISBN 84-7820-848-8, pags. 353–362, Jan. 2006.
[44] D. Ajò, U. Casellato, E. Fiorin, P.A. Vigato, Ciro Ferri's frescoes: a study of painting materials and technique by SEM-EDS microscopy, X-ray diffraction, micro FT-IR and photoluminescence spectroscopy, J. Cult. Herit. 5 (4) (2004) 333–348, doi:10.1016/j.culher.2004.05.003.
[45] H. Wilkens, On artificial Ultramarine, J Frankl. Inst 35 (1858) 136–138 10.59.
[46] S.M. Aleksandrov, V.G. Senin, Genesis and composition of lazurite in magnesian skarns, Geochem. Int. 44 (10) (2006) 976–988, doi:10.1134/S001670290610003X.
[47] A. Mangone, M.C. Caggiani, T. Forleo, L.C. Giannossa, P. Acquafredda, A possible natural and inexpensive substitute for lapis lazuli in the Frederick II era: The finding of haüyne in blue lead-tin glazed pottery from Melfi Castle (Italy), Molecules 28 (4) (2023), doi:10.3390/molecules28041546.